Available online at www.sciencedirect.com

ScienceDirect

Ceramics International 41 (2015) 14754–14759

CERAMICS INTERNATIONAL

www.elsevier.com/locate/ceramint

Spherical assemblies of titania nanotubes generated through aerosol processing

Dragana J. Jovanović[a], Ivan M. Dugandžić[b], Gordana Ćirić-Marjanović[c], Tamara Radetić[d], Scott P. Ahrenkiel[e], Olivera B. Milošević[b], Jovan M. Nedeljković[a], Zoran V. Šaponjić[a,*], Lidija T. Mancic[b,**]

[a]*Vinča Institute of Nuclear Sciences, University of Belgrade, P.O. Box 522, 11001 Belgrade, Serbia*
[b]*Institute of Technical Sciences of SASA, Knez Mihailova 35/IV, 11000 Belgrade, Serbia*
[c]*Faculty of Physical Chemistry, University of Belgrade, Studentski Trg 12-16, 11158 Belgrade, Serbia*
[d]*Faculty of Technology and Metallurgy, University of Belgrade, Karnegijeva 4, 11120 Belgrade, Serbia*
[e]*South Dakota School of Mines and Technology, 501 E. Saint Joseph Street, Rapid City, SD 57701, USA*

Received 22 June 2015; received in revised form 25 July 2015; accepted 29 July 2015
Available online 7 August 2015

Abstract

We report on the possibility to build hierarchically organized three-dimensional (3D) titania spherical particles having high surface-to-volume-ratio, by aerosol processing of nanotubular building blocks. Morphology and crystal structure of titania based spherical assemblies, obtained in the temperature range from 150 to 650 °C, were characterized by means of scanning and transmission electron microscopy, x-ray powder diffraction and Raman spectroscopy. Initial shape of 1D building units, nanotubes, was well preserved in the spherical assemblies processed at 150 and 450 °C. Processing at 650 °C resulted in a collapse of the nanotubular building blocks and formation of the assemblies of irregularly shaped TiO_2 nanoparticles. Structural analysis revealed several phase transitions in titania spherical assemblies in course with the temperature increase indicating possibility of in-situ phase composition adjustment during aerosol processing.

Keywords: A. Ultrasonic techniques; B. Electron microscopy (TEM and SEM); B. Raman spectroscopy and scattering; D. TiO_2

1. Introduction

The ability of systematic manipulation of size and shape of metal-oxide nanoparticles opens up new possibilities to control their optical, electrical, photocatalytic and chemical properties. Synthesis and characterization of axially anisotropic nano-objects (1D) such as nanotubes and nanorods has been well studied [1]. Recently, significant scientific and technological interests have been directed toward synthesis of microspherical materials based on the 1D nanoscale building blocks. Various soft chemistry and chemical vapor deposition methods have been employed for generation of the hierarchical microspherical structures based on the 1D nanoscale building blocks [2]. Despite to the numerous published studies, new designs of titania based materials in hierarchically organized assemblies are still very attractive, since it results in synergy of different shape- and size-based functional properties that have promising application in solving major energy and environmental issues [2,3]. As it is well known, titanium dioxide (TiO_2) is a semiconductor with variety of applications in heterogeneous catalysis [4], photocatalysis [5], solar cells [6,7], production of hydrogen, ceramics, gas-sensors [8] and smart textile materials with antibacterial and self-cleaning properties [9]. In the form of a micro- or mesoporous material anatase TiO_2 could be used as an electrolyte in Proton Exchange Membrane Fuel Cells (PEMFC) [10]. Additionally, axially anisotropic nano-objects, such as scrolled titania nanotubes, represent a new class of materials characterized by unique surface structure accessible for surface

*Corresponding author. Tel.: +381113408277; fax: +381113408 607.
**Corresponding author. Tel.: +381112185437; fax: +381112185263.
E-mail addresses: saponjic@vinca.rs (Z.V. Šaponjić), lidija.mancic@itn.sanu.ac.rs (L.T. Mancic).

http://dx.doi.org/10.1016/j.ceramint.2015.07.205
0272-8842/

modification with oxygen-containing ligands, and finally capable of efficient light harvesting and photoinduced charge separation [11]. Recently, it was shown that spherical aggregates of such nano-objects, fabricated through three different processing steps, is promising material for dye sensitized solar cells exhibiting the high energy conversion efficiency [12].

In our previous work we showed that the aerosol processing is a suitable method for processing of colloidal TiO_2 nanoparticles which results in the formation of submicronic TiO_2 spheres [13]. Recently, we applied this method under specific conditions which enabled generation of hierarchically organized spherical TiO_2 particles with preserved surface structure of clustered building units (45-Å TiO_2 nanoparticles) [14]. Such surface structure allows for the modification with various ligands (dopamine, catechol, 2,3-dihydroxynaphthalene and anthrarobin) and formation of the charge-transfer complexes resulting in extended optical absorption in the visible spectral region [14,15].

This paper is the first report, to the best of our knowledge, on assembling of colloidal titania nanotubes into hierarchical superstructure, i.e., non-agglomerated submicron spheres thorough application of the aerosol processing. Both morphology and crystal structure of the spherical assemblies obtained at different temperatures were thoroughly characterized and discussed.

2. Materials and methods

Dispersion of short titania nanotubes used as a precursor for aerosol processing was prepared according to Kasuga et al. [16]. The 250 mg of Degussa TiO_2 powder was dispersed in 10 ml 10 M NaOH and hydrothermally treated 24 h in a Teflon vessel (total volume 25 ml) under saturated vapor pressure of water at 150 °C. After autoclaving, the ensuing powder was sequentially washed with a 0.1 M HCl and H_2O up to pH 7. After each washing cycle supernatant was separated from the powder by centrifugation. The collected supernatant containing the short nanotubes and large excess of exchange ions was roughly dialyzed against distilled water. The resulted purified dispersion of short nanotubes was used further as a precursor for aerosol processing of submicron titania spherical assemblies. The concentration of Ti^{4+} ions in dispersion of short nanotubes was 174.4 ± 0.5 ppm as determined by ICP Emission Spectrometer: ICAP 6000 series (Thermo Electron Corporation).

The dispersion consisting of nanotubes was ultrasonically atomized (1.3 MHz) in a three-zone tubular flow reactor using a nitrogen flow of 2 dm^3/min. The mean value of the atomized droplet size, calculated by Lang equation [17], was 3.3 μm. For the processing temperatures of 150, 450 and 650 °C, calculated droplet to particle conversion times were 23, 13 and 10 s, respectively [18] while the calculated mean particle size was 200 nm [19]. Obtained powders were collected in the electrostatic precipitator. A schematic of the laboratory set-up was presented in our previous work [20].

The morphology and chemical composition of nanotubular precursor and spherical assemblies were characterized using scanning electron microscopy (Philips XL30 SEM/EDS) and transmission electron microscopy (JEOL-TEM 2100 LaB_6 operated at 200 kV and JEOL 100 CX operating at 100 kV). The measurements of the nanotube length, inner and outer diameters were performed on the TEM images, while the mean sizes of the synthesized spherical assemblies were determined from SEM images using ImageJ software.

Structural characterization of all samples by X-ray powder diffraction (XRPD) was performed using X'Pert Philips powder diffractometer with Cu Kα radiation. The XRPD patterns were recorded in the 2θ range of 5–90° with a step size of 0.02° and accounting time of 11 s per step. Unit cell parameters were determined using Lebail refinement [21] in Topas Academic 4.1 [22].

Raman spectra excited by a diode-pumped solid-state 532 nm laser (laser power of 3–5 mW on a specimen) were collected on a Thermo Scientific DXR Raman microscope, equipped with a research optical microscope and a CCD detector.

3. Results and discussion

Colloidal titania based nanotubular precursor is made up of open-ended, short free-standing multi-wall nanotubes, Fig. 1. Dimensions of the nanotubes: inner and outer diameters, as well as length, were estimated to be 6.5 ± 0.5, 10.5 ± 1.2 and 78.7 ± 15.3 nm, respectively. The corresponding interlayer spacing of 7.9 Å within the nanotubes wall (marked region

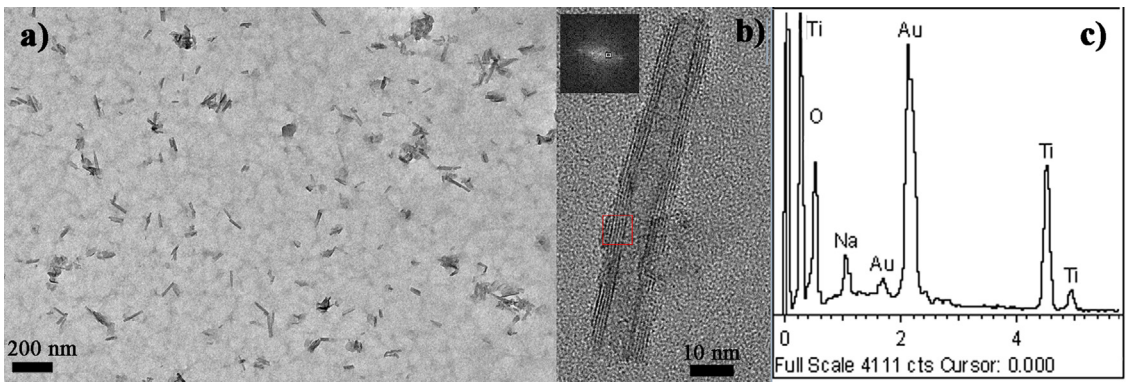

Fig. 1. Typical TEM images of the colloidal nanotubular precursor (a), at higher magnification (b) and corresponding EDS spectra obtained from SEM measurements (c).

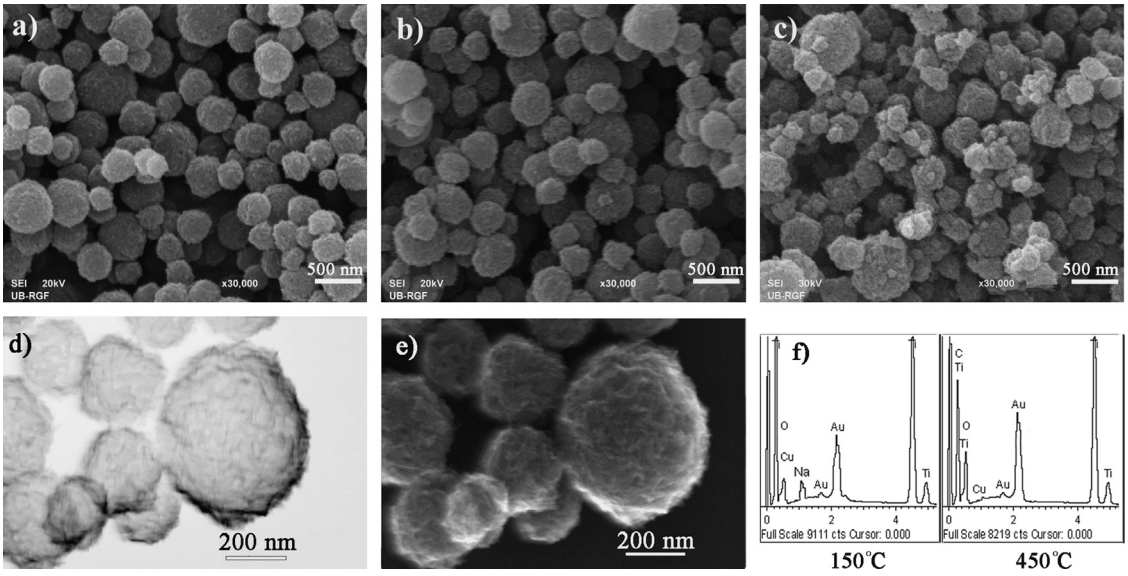

Fig. 2. Typical SEM images of spherical assemblies processed at 150 °C (a), 450 °C (b), 650 °C (c), 150 °C in BEI-TOPO mode (d), 150 °C in BEI-COMPO mode (e) and EDS spectra of spherical assemblies processed at 150 and 450 °C (f).

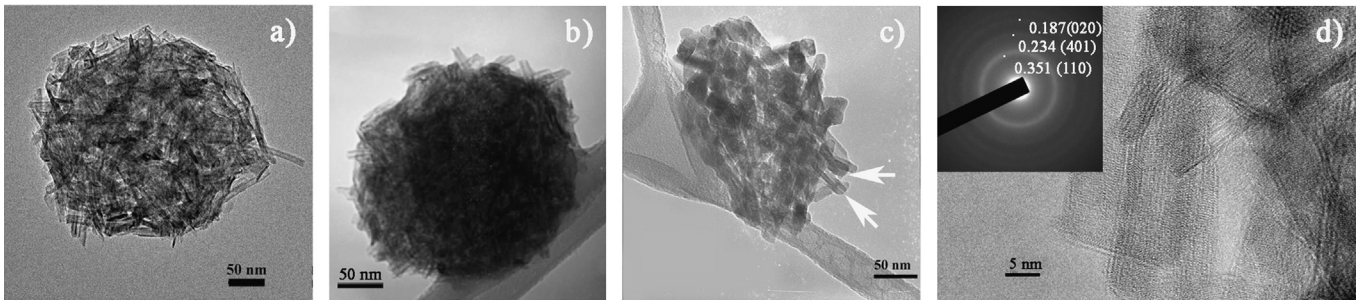

Fig. 3. Typical TEM images of spherical assemblies processed at 150 °C (a), 450 °C (b), 650 °C (c), and TEM image (higher magnification) of spherical assembly processed at 150 °C, inset: SAED pattern with corresponding crystal planes (distances in nm) (d).

in Fig. 1b) was determined by applying Fast Fourier Transformation (FFT), given as an inset at the same figure. The EDS spectrum, Fig. 1c, showed that certain degree of sodium was retained in the tubular precursor after washing and dialysis.

Aerosol processing of the dispersion of titania nanotubes at different temperatures resulted in formation of the non-agglomerated particles i.e. spherical assemblies with dimensions in the range from 160 to 650 nm, Fig. 2a–c. From the normal (Gaussian) type of particles size distribution (not shown) mean particle sizes of 360, 340 and 300 nm were obtained for powders synthesized at 150, 450 and 650 °C, respectively. For the experimental conditions applied in this work, by calculation predicted particle size should be 200 nm (assuming generation of dense particle) which is a considerably lower than experimentally achieved one indicating generation of loosely packed particles at all processing temperatures. Rough surface of the spherical assemblies fits well with this, since that the presence of well-defined sub-structural building units is clearly notable. In addition, two types of information contained in the backscattered electron image (BEI) could be separated by electronically pairing of the opposing quadrants revealing particle topography (BEI TOPO) and composition (BEI COMPO). SEM image recorded in BEI TOPO mode, Fig. 2d, confirmed roughness and indicated certain level of particles porosity (darker fields). SEM image recorded in BEI COMPO mode, Fig. 2e, revealed particles compositional homogeneity. The EDS spectra, Fig. 2f, indicated decrease in sodium content with increasing processing temperature.

TEM characterization revealed that the nanotubular morphologies of the building blocks were solely preserved in the spherical assemblies processed at lower temperatures, Fig. 3a and b. Open-ended nanotubes (marked with arrows) were detected even in the samples processed at the highest temperature (650 °C), although for that processing condition sub-structural units are dominantly nanoparticles, Fig. 3c. In all samples, Fig. 3a–c, particle porosity is noticeable due randomly established interconnectivity of the constituent building blocks. TEM image at higher magnification with a corresponding SAED pattern (Fig. 3d) reveals polycrystalline nature of the spherical assembly processed at 150 °C and suggests formation of TiO_2 (B) phase, since that observed rings match the positions of the (110), (401) and (020) crystal planes reported in its reference pattern (PDF 74-1940, Monoclinic, C2/m).

Crystalline structure of the nanotubes used as the precursor is usually assigned as quasi-anatase or partially proton-exchanged sodium titanates [23]. The XRPD patterns of the nanotubular

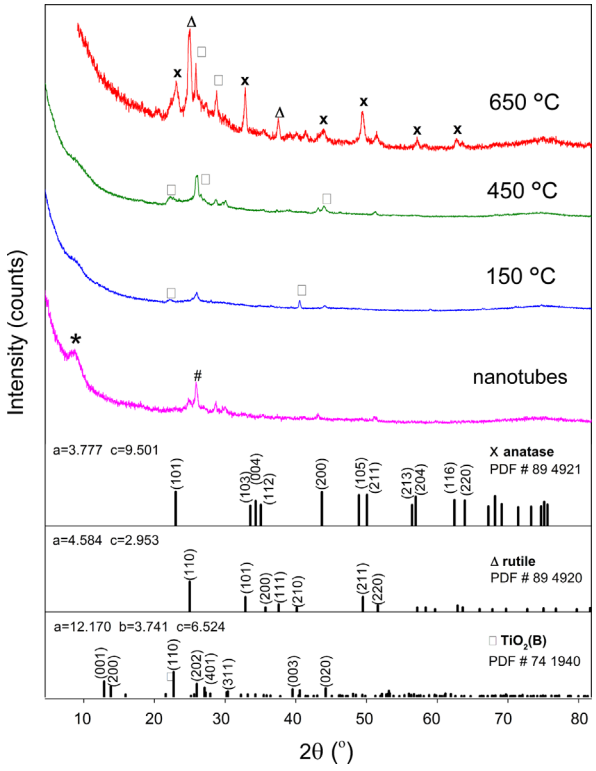

Fig. 4. X-ray powder diffraction patterns of the nanotubular precursor and the spherical assemblies formed by aerosol processing at 150, 450 and 650 °C. Bragg peak positions and corresponding unit cell parameters (in Å) of anatase, rutile and TiO_2(B) phases are included for the reference. The diffraction peak at $2\theta=9.17^\circ$ in the XRPD pattern of short nanotubes (marked with *) corresponds to their interlayer distance of $d=9.6$ Å. The diffraction peak at $2\theta=28.5^\circ$ (marked with), is a "fingerprint" reflection of a monoclinic $Na_{2-x}H_xTi_3O_7 \cdot nH_2O$ phase [24].

precursor and the spherical assemblies generated by the aerosol processing at different temperatures are presented in Fig. 4. The diffraction peak at $2\theta=9.17^\circ$ ($d=9.6$ Å) in the XRPD pattern of short nanotubes (marked with * in Fig. 4) corresponds to their interlayer distance.

The absence of the main anatase diffraction line at $2\theta=25.3^\circ$ and appearance of a peak at $2\theta=28.5^\circ$ (marked with), a "fingerprint" reflection of a monoclinic $Na_{2-x}H_xTi_3O_7 \cdot nH_2O$ phase [24], imply that nanotubular precursor has trititanate layered structure. As it is shown previously, intensity and position of the first peak at $2\theta\sim10^o$ depends on the level of the proton exchange and the amount of the intercalated water [25]. The difference between the values observed by XRPD, Fig. 4, and FFT from TEM, Fig. 1b, is just due to the high vacuum in the TEM chamber and consequent severe dehydration. The broad reflection at $2\theta=24.5^\circ$ ($d=3.5$ Å) in powders processed at the lower temperatures (150 and 450 °C) confirms the formation of monoclinic TiO_2 (B) phase (PDF 74-1940; Monoclinic, C2/m), whose presence was indicated by electron diffraction measurements, inset in Fig. 3d. On the other hand, characteristic peaks of anatase at $2\theta=25.3^\circ$ (PDF 89-4921; Tetragonal, $I4_1/amd$) and rutile at $2\theta=27.5^\circ$ (PDF 89-4920; Tetragonal, $P4_2/mnm$) were observed in assemblies obtained at the highest temperature (650 °C). According to the literature [24,26], the appearance of the TiO_2(B), before anatase formation, is a consequence of the thermal decomposition of proton exchanged titanates ($H_2Ti_nO_{2n+1}$ $(3\le n\le 6)$) whose existence is in agreement with a low sodium content detected by EDS, in the spherical assemblies processed at 450 °C, Fig. 2f. The refined lattice parameter values (in Å) for the detected TiO_2 structures were: $a=12.174(3)$ $b=3.712(1)$ $c=6.523(3)$ for TiO_2(B); $a=3.768(4)$ $c=9.482(1)$ for anatase; and $a=4.590(1)$ $c=2.947(1)$ for rutile. They are comparable with the values of the reference crystal cell parameters reported in Fig. 4.

Having in mind high sensitivity of Raman spectroscopy for detecting specific crystal phases [27], Raman spectra of nanotubular titania precursor and their spherical assemblies obtained by aerosol processing were measured, Fig. 5. Raman spectra of the titania nanotubes displays broadening of the bands, Fig. 5, in contrast to the sharp Raman bands characteristic for the raw TiO_2 based materials [28,29]. The bands at wavenumbers 141 (vs), 182 (w), 384 (w) and 507 cm^{-1} (w), Fig. 5, are downshifted slightly with respect to the corresponding bands in the spectrum of pure anatase at 144, 197, 399, and 513 cm^{-1} [28,30]. The presence of the anatase E_g phonon mode in the spectrum of nanotubes at 141 cm^{-1} demonstrates that the tetrahedral structure formed in nanotubes is preserved [28]. Appearance of new bands in the spectrum of the precursor nanotubes at 273 (vs), 441 (vs), 605 (m), 655 (m-s), 694 (m), 769 (w), 808 (w) and 913 cm^{-1} (m), can be

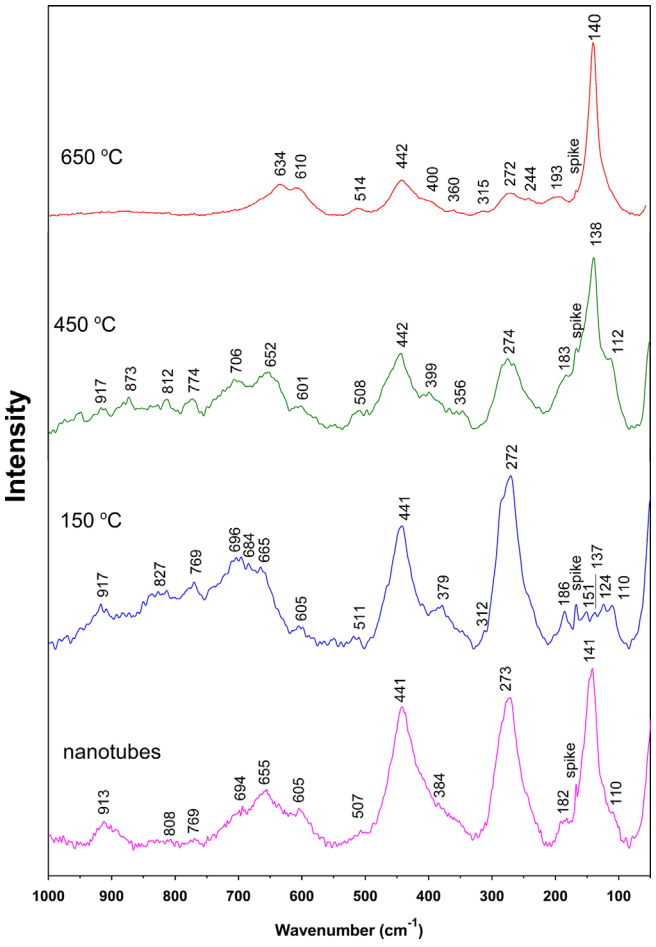

Fig. 5. Raman spectra of the nanotubular precursor and the spherical assemblies formed by aerosol processing at 150, 450 and 650 °C.

related to the changes in TiO_2 from three-dimensional crystallites to two-dimensional sheets although their exact assignment is still under dispute [31]. The Raman band at about 274 cm^{-1} has been recognized in the literature as an intrinsic mode related to the sodium titanates, i.e. to the Ti–O vibration affected by the sodium ion in the near vicinity [28], while the band at 441 cm^{-1} is attributed to the Ti–O–Ti crystal phonons [32]. The broad band observed at 655 cm^{-1} corresponds to the Ti–O–Ti band vibrations and is previously observed for titanate nanotubes at 668 cm^{-1} [32]. The band at 913 cm^{-1} is also typically observed for 1D titanates and is assigned to ν(Ti–O) modes, which involve non-bridging oxygen atoms at the corners of TiO_6 slabs [33].

Raman spectra of the titania assembles prepared at different temperatures showed that there is a change of the intensity ratio for the three main Raman bands at 441, 273 and 141 cm^{-1}. That is an indication of fine changes in nanotubular structure. Disappearance of the very strong E_g band at 141 cm^{-1} and appearance of weak bands at 124, 137 and 151 cm^{-1} in the spectrum of the assemblies processed at 150 °C points to changes in the tetrahedral structure. According to literature data [27,34], these bands could be assigned to the δ(O–Ti–O) and δ(Ti–O–Ti) vibration modes of TiO_2 (B) polymorph, which is in agreement with the appearance of reflection at 2θ=24.5° in the corresponding XRPD pattern.

Titania assemblies obtained at 450 °C have a much stronger band at 138 cm^{-1} compared to samples processed at a lower temperature (150 °C). It could be the consequence of the re-appearance of anatase E_g phonon mode that overlaps TiO_2 (B) modes in the range from the 100 to 200 cm^{-1} [27]. The intensity of Raman bands related to titanates at 274 and 441 cm^{-1} was observed to decrease. The Raman spectrum of the spherical assemblies synthesized at 650 °C is significantly different from the other two spectra, which is in accordance with the TEM and XRPD results (Figs. 3 and 4). The band at 140 cm^{-1} becomes particularly strong and dominating in the spectrum, while the bands at 442 and 272 cm^{-1}, characteristic for titania nanotubes further decreased, indicating the increased content of anatase TiO_2 in this sample. The high content of anatase phase in this assembly is supported by the appearance of new band at 634 cm^{-1}, which corresponds well to the E_g mode of pure anatase at ~639 cm^{-1} [28], as well as by the bands at 193, 400 and 514 cm^{-1} whose positions correspond well to those of pure anatase at 197, 399 and 513 cm^{-1}, respectively. The presence of rutile phase, indicated by XRPD analysis, in titania assemblies prepared at 650 °C is also supported Raman spectroscopy. The appearance of new band at 244 cm^{-1}, specific feature of rutile was observed [35,36], as well as the enhancement and shifting of the band observed at 601/605 cm^{-1} in the spectra of the other samples, to 610 cm^{-1}. Band at 610 cm^{-1} is very close to the position of A_{1g} mode of pure rutile at 612 cm^{-1} [28,35,36].

4. Conclusions

Aerosol processing proved to be suitable method for generation of non-agglomerated submicronic titania spherical assemblies from colloidal 1D nanotubular precursor. The advantage of the reported method relies on the fact that the morphology, size and phase composition of hierarchical 3D structures could be controlled simply by varying the processing temperatures. The morphology of nanotubular building blocks was preserved in spherical assemblies processed at temperatures up to 450 °C, while collapsing of nanotubes was detected in assemblies formed at 650 °C. Alteration of aerosol processing temperatures induced generation of different TiO_2 polymorphs (TiO_2(B), anatase and rutile) as it is confirmed by XRPD, SAED and Raman spectroscopy. Aerosol processing of 1D nano-building units opens up possibilities for the synthesis of a new class of materials.

Acknowledgments

The financial support for this work was provided by the Ministry of Education, Science and Technological Development of Republic of Serbia (Projects 45020, 172056 and 172043). The work is done under the umbrella of COST Action MP1106. The authors are grateful to Prof. Maria Eugenia Rabanal, University Carlos III, Madrid, Spain for XRD measurements.

References

[1] Z. Zheng, B. Huang, X. Qin, X. Zhang, Y. Dai, Strategic synthesis of hierarchical TiO_2 microspheres with enhanced photocatalytic activity, Chem. Eur. J. 16 (2010) 11266–11270.
[2] Z. Ren, Y. Guo, C.-H. Liu, P.-X. Gao, Hierarchically nanostructured materials for sustainable environmental applications, Front. Chem. 1 (18) (2013) 1–22.
[3] G. Neri, A. Bonavita, G. Micali, G. Centi, S. Perathoner, R. Passalacqua, M.C. Willinger, N. Pinna, Synthesis, characterization and sensing applications of nanotubular TiO_2-based materials, Lect. Notes Electr. Eng. 91 (2011) 151–154.
[4] M.J. López-Muñoz, J. Aguado, A. Arencibia, R. Pascual, Mercury removal from aqueous solutions of $HgCl_2$ by heterogeneous photocatalysis with TiO_2, Appl. Catal. B 104 (2011) 220–228.
[5] C. Wang, T. Wu, TiO_2 nanoparticles with efficient photocatalytic activity towards gaseous benzene degradation, Ceram. Int. 41 (2015) 2836–2839.
[6] M. Grätzel, Dye-sensitized solar cells, J. Photochem. Photobiol. C 4 (2003) 145–153.
[7] M.S. Liang, C.C. Khaw, C.C. Liu, S.P. Chin, J. Wang, H. Li, Synthesis and characterization of thin-film TiO_2 dye-sensitized solar cell, Ceram. Int. 39 (2013) 1519–1523.
[8] U. Diebold, The surface science of titanium dioxide, Surf. Sci. Rep. 48 (2003) 53–229.
[9] D. Mihailović, Z. Šaponjić, M. Radoičić, T. Radetić, P. Jovančić, J. Nedeljković, M. Radetić, Functionalization of polyester fabrics with alginates and TiO_2 nanoparticles, Carbohydr. Polym. 79 (2010) 526–532.
[10] M.T. Colomer, Nanoporous anatase thin films as fast proton-conducting materials, Adv. Mater. 18 (3) (2006) 371–374.
[11] Z.V. Šaponjić, N.M. Dimitrijevic, D.M. Tiede, A.J. Goshe, X. Zuo, L.X. Chen, A.S. Barnard, P. Zapol, L. Curtiss, T. Rajh, Shaping nanometer-scale architecture through surface chemistry, Adv. Mater. 17 (8) (2005) 965–971.
[12] Z. Liu, X. Su, G. Hou, S. Bi, Z. Xiao, H. Jia, Spherical TiO_2 aggregates with different building units for dye-sensitized solar cells, Nanoscale 5 (2013) 8177–8183.
[13] J.M. Nedeljković, Z.V. Šaponjić, Z. Rakočević, V. Jokanović, D.P. Uskoković, Ultrasonic spray pyrolysis of TiO_2 nanoparticles, NanoStruct. Mater. 9 (1997) 125–128.
[14] I.M. Dugandžić, D.J. Jovanović, L. Mančić, N. Zheng, S.P. Ahrenkiel, O. Milošević, Z.V. Šaponjić, J.M. Nedeljković, Surface modification of

submicronic TiO_2 particles prepared by ultrasonic spray pyrolysis for visible light absorption, J. Nanopart. Res. 14 (2012) 1157–1167.
[15] I.M. Dugandžić, D.J. Jovanović, L.T. Mančić, O.B. Milošević, S.P. Ahrenkiel, Z.V. Šaponjić, J.M. Nedeljković, Ultrasonic spray pyrolysis of surface modified TiO_2 nanoparticles with dopamine, Mater. Chem. Phys. 143 (2013) 233–239.
[16] T. Kasuga, M. Hiramatsu, A. Hoson, T. Sekino, K. Niihara, Formation of titanium oxide nanotube, Langmuir 14 (1998) 3160–3163.
[17] R.J. Lang, Ultrasonic atomization of liquids, J. Acoust. Soc. Am. 34 (1) (1962) 6–8.
[18] W.N. Wang, Y. Kaihatsu, F. Iskandar, K. Okuyama, Highly luminous hollow chloroapatite phosphors formed by a template-free aerosol route for solid-state lighting, Chem. Mater. 21 (19) (2009) 4685–4690.
[19] W. Widiyastuti, W.-N. Wang, I.W. Lenggoro, F. Iskandar, K. Okuyama, Simulation and experimental study of spray pyrolysis of polydispersed droplets, J. Mater. Res. 22 (2007) 1888–1898.
[20] O. Milošević, L. Mančić, M.E. Rabanal, L.S. Gomez, K. Marinković, Aerosol route in processing of nanostructured functional materials, KONA Powder Part. J. 27 (2009) 84–106.
[21] A. LeBail, Whole powder pattern decomposition methods and applications: a retrospection, Powder Diffr. 20 (2005) 316–326.
[22] A.A. Coelho, 2004 TOPAS-Academic.
[23] D.V. Bavykin, F.C. Walsh, Titanate and Titania Nanotubes: Synthesis, Properties and Applications, R.S.C., Nanoscience and Nanotechnology No.12, Cambridge, UK, 2009.
[24] E. Morgado Jr, M.A.S. De Abreu, O.R.C. Pravia, B.A. Marinkovic, P.M. Jardim, F.C. Rizzo, A.S. Araújo, A study on the structure and thermal stability of titanate nanotubes as a function of sodium content, Solid State Sci. 8 (2006) 888–900.
[25] P. Pontón, J.R. d'Almeida, J. Roberto, B. Marinkovic, S. Savic, L. Mancic, N. Rey, E. Morgado Jr., F. Rizzo, The effects of the chemical composition of titanate nanotubes and solvent type on 3-aminopropyltriethoxysilane grafting efficiency, Appl. Surf. Sci. 301 (2014) 315–322.
[26] L. Mancic, I. Dugandzic, O. Milosevic, D. Jovanovic, Z. Saponjic, M.E. Rabanal, L. Gomez, Aerosol-assisted processing of hierarchically organized TiO_2 nanoparticles, IJMPT 50 (3–4) (2015) 221–229.
[27] T. Beuvier, M. Richard-Plouet, L. Brohan, Accurate methods for quantifying the relative ratio of anatase and TiO_2(B) nanoparticles, J. Phys. Chem. C 113 (2009) 13703–13706.
[28] L. Qian, Z.L. Du, S.Y. Yang, Z.S. Jin, Raman study of titania nanotube by soft chemical process, J. Mol. Struct. 749 (2005) 103–107.
[29] T. Gao, H. Fjellvåg, P. Norby, Crystal structures of titanate nanotubes: a Raman scattering study, Inorg. Chem. 48 (2009) 1423–1432.
[30] R.T. Downs, The RRUFF Project: an integrated study of the chemistry, crystallography, Raman and infrared spectroscopy of mineral; RRUFF ID: R060277, in: Proceedings of the Program and Abstracts of the 19th General Meeting of the International Mineralogical Association in Kobe, Japan, 2006, O03-O13, ⟨http://www.fis.unipr.it/phevix/ramandb.php⟩.
[31] B.D. Yao, Y.F. Chan, X.Y. Zhang, W.F. Zhang, Z.Y. Yang, N. Wang, Formation mechanism of TiO_2 nanotubes, Appl. Phys. Lett. 82 (2003) 281–283.
[32] D.V. Bavykin, J.M. Friedrich, A.A. Lapkin, F.C. Walsh, Stability of aqueous suspensions of titanate nanotubes, Chem. Mater. 18 (2006) 1124–1129.
[33] X. Sun, Y. Li, Synthesis and characterization of ion-exchangeable titanate nanotubes, Chem. Eur. J 9 (2003) 2229–2238.
[34] M.B. Yahia, F. Lemoigno, T. Beuvier, J.-S. Filhol, M. Richard-Plouet, L. Brohan, M.-L. Doublet, Updated references for the structural, electronic, and vibrational properties of TiO_2(B) bulk using first-principles density functional theory calculations, J. Chem. Phys. 130 (2009) 204501.
[35] O. Frank, M. Zukalova, B. Laskova, J. Kürti, J. Koltai, L. Kavan, Raman spectra of titanium dioxide (anatase, rutile) with identified oxygen isotopes (16, 17, 18), Phys. Chem. Chem. Phys. 14 (2012) 14567–14572.
[36] Mineral Raman DataBase, Rutile 1, ⟨http://www.fis.unipr.it/phevix/ramandb.html⟩.